review article

Nuclear vibrations

G. F. Bertsch
Michigan State University, East Lansing, Michigan 48824

Three types of nuclear vibrations have been observed in which a large fraction of the nucleons participate. There is a satisfactory explanation for the vibrational frequencies but not for the damping rates.

NUCLEI, like more familiar mechanical systems, can undergo simple vibratory motions. One mode of motion, in which protons move together in one direction while the neutrons simultaneously move in the opposite direction, has been known for 30 years. In the past decade, several new vibrational modes have been discovered. Our theoretical understanding of the nuclear motion has also considerably advanced. Although the most refined descriptions of the motion require a quantum many-body theory, the main features of the vibrations can be understood using classical physics. The motion of an extended body is described by a field of vectors which give the velocity of the medium at each point. Figure 1 shows the velocity fields for three types of vibration: monopole, dipole and quadrupole. These three modes are exhibited by nuclei as so-called 'giant vibrations', in which a large fraction of the nucleons participate in the motion. In both the monopole and quadrupole modes, all the nucleons move coherently in a direction which depends on their position in the nucleus. In the dipole motion, as mentioned above, protons and neutrons move in opposite directions.

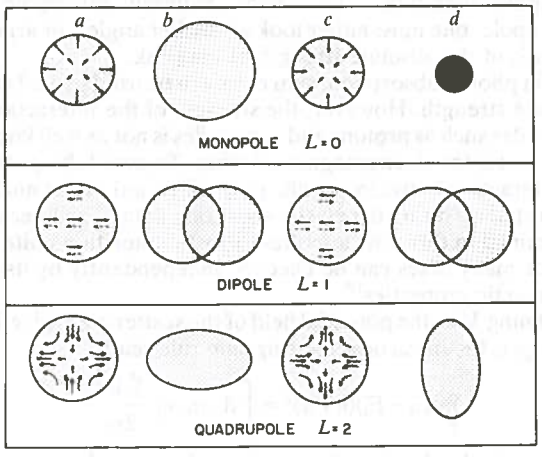

Fig. 1 The cycle of oscillation for simple vibrations. The velocity field at the moment when the nucleus passes through the equilibrium shape is shown in *a* and *c*. The shape at maximum distortion is shown in *b* and *d*. For the dipole, the neutrons and protons move in opposite directions. For other modes, the neutrons move with protons.

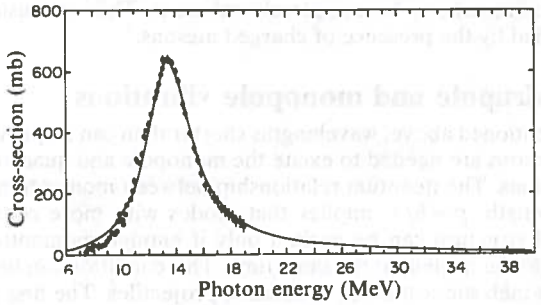

Fig. 2 The giant dipole resonance in ^{208}Pb, as observed by the photon reaction cross section (ref. 3, Fig. 32). The points are the experimental data, and the curve is the lorentzian function.

Dipole vibration

The first nuclear vibration to be observed, the giant dipole, was found in measurements of photon absorption. The reaction cross-section is enhanced by resonance when the photon frequency matches the vibrational frequency. The first indications of the giant dipole resonance were obtained before photon beams with a broad energy range were available. Bothe and Gentner in 1937 had a source of 14 MeV photons and they measured the radioactivity produced in a variety of targets[1]. The cross-sections varied considerably from target to target, indicating that there was a resonant absorption in some of the targets. By the mid-1940s, electron accelerators became available which produced bremsstrahlung photon beams of sufficient energy to observe the resonance. The improved data[2] showed that the absorption was concentrated in a resonance, the frequency of which varied systematically with the size of the nucleus.

One problem with these measurements is that the bremsstrahlung beam is broadly distributed in energy, so that the measurement for a particular energy required careful subtraction techniques. Currently, these experiments are done with photons that are produced by annihilation of positron, and are therefore monoenergetic. An example of the data now available[3] with this improved technique is shown in Fig. 2. The points are experimental data, and the curve is the lorentzian distribution,

$$\sigma(E)=\frac{\sigma_m}{1+[(E^2-E_m^2)^2/E^2\Gamma^2]}$$

0028-0836/79/340639-06$01.00

This formula has three parameters: a maximum strength σ_m, a centre frequency E_m, and a damping width Γ, which are adjusted to fit the data. For the heavier nuclei, the frequency depends on nuclear mass number A roughly as $\hbar\omega = 80/A^{1/3}$ MeV. The damping width is 4–5 MeV.

The spatial structure of the vibration, with protons moving against neutrons, is inferred indirectly from the data. Photons at the frequencies of interest have a long wavelength (~100 fm) on the scale of nuclear dimensions $R \sim 1.2\,A^{1/3} \sim 3$–$8$ fm. With a long wavelength, the force field is quite uniform and the photons cannot excite other kinds of motion besides the uniform displacement of protons against neutrons. Thus, as is the case with optical photons interacting with atoms, all but a negligible fraction of the cross-section is due to dipolar motion. It is useful to compare the magnitude of the cross-section with a theoretical limit known as a sum rule. The Thomas–Reiche–Kuhn sum rule for the absorption is given by[4]

$$\int_0^\infty \sigma(\omega)\,\mathrm{d}\omega = \frac{2\pi^2 e^2}{Mc}\,\frac{NZ}{A}$$

where M is the mass of a nucleon, and N, Z are the neutron and proton numbers. The dipole vibration will satisfy this sum rule only if all the protons move coherently with a uniform translation. In the example shown in Fig. 2, the experimental absorption strength from the lorentzian fit is 3,000 MeV mb, which is just the limit from the sum rule. Thus, the motion in the dipole vibration seems to be completely coherent. This conclusion is modified by the presence of charged mesons.[5]

Quadrupole and monopole vibrations

As mentioned above, wavelengths shorter than can be provided by photons are needed to excite the monopole and quadrupole vibrations. The quantum relationship between momentum and wavelength, $p = h/\lambda$, implies that modes with more complex spatial structure can be excited only if enough momentum is given to the nucleus at the same time. This condition can be met by the inelastic scattering of massive projectiles. The first published experiments exhibiting a new vibration were done in 1957 with inelastic proton scattering at 180 MeV (ref. 6). Figure 3 shows these data; a distinct bump is visible at 18 MeV excitation. However, the significance of this bump was not realised until in 1971, when Bertrand and coworkers[7] found the bump in their own data taken at lower energies and concluded that it was the quadrupole vibration of Fig. 1. Others also saw the vibration in electron scattering[8], and offered a quadrupole vibration as one of the possible explanations.

The main evidence that the bump might be a quadrupole vibration was the angular distribution of the scattering cross-section. Each multipolarity has a characteristic shape to the angular distribution, which can be calculated by the Schrödinger equation for the projectile wavefunction. If the wavelength of the projectile is short compared to the dimensions of the target,

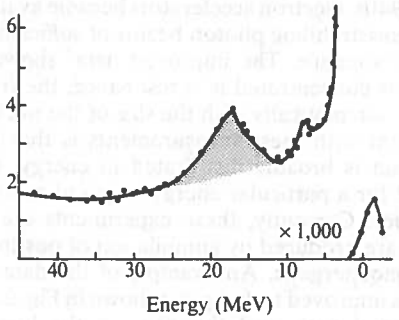

Fig. 3 Inelastic proton scattering spectrum for 180 MeV protons on a Ca target (ref. 5, Fig. 2). The stippled bump is the quadrupole vibration. The rise in cross-section towards zero excitation energy is the elastic scattering.

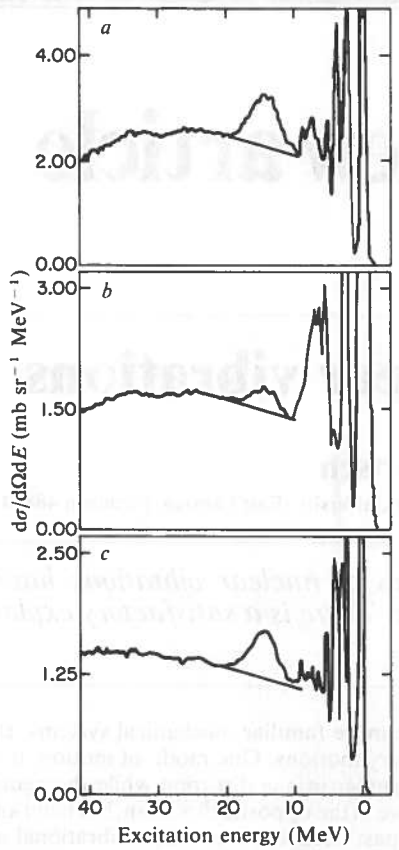

Fig. 4 Inelastic α-particle scattering on ^{90}Zr, taken at three different angles. *a*, $\theta_{lab} = 17.5°$; *b*, $\theta_{lab} = 20.5°$; *c*, $\theta_{lab} = 22.5°$. The giant quadrupole is prominent at 17.5° and 22.5°, but is much reduced at 20.5° (ref. 9).

the angular distribution peaks at an angle given roughly by $\theta = L/\lambda R$, where L is the multipolarity of the excitation and R is the nuclear radius. At larger angles, the cross-section is oscillatory, with interference from the projectile passing opposite sides of the nucleus. Some recent data with angular dependence is shown in Fig. 4[9].

The reaction is induced by α particles scattering on the nucleus ^{90}Zr. A prominent peak is seen at angles of 17.5° and 22.5°, but much reduced at 20.5°. This behaviour is only consistent with the predicted angular distributions for quadrupole or monopole vibrations. To decide between monopole and quadrupole, one must either look at smaller angles, or argue on the basis of the absolute strength of the peak.

As in photon absorption, sum rules can be used to analyse the absolute strength. However, the strength of the interaction for projectiles such as protons and α particles is not as well known *a priori* as it is for electromagnetic probes. To avoid this problem, the interaction between specific projectiles and target nucleons is adjusted by fitting the elastic scattering data. The interaction determined in this way describes inelastic transition quite well, and for many cases can be checked independently by its electromagnetic properties[10].

Defining V as the potential field of the scattering projectile on the target, the inelastic scattering sum rule reads

$$\sum_f (E_f - E_i)\langle i|V|f\rangle^2 = \int \mathrm{d}^3 r n_0(r)\,\frac{(\vec{\nabla}V)^2}{2m}$$

where n_0 is the density of nucleons in the ground state and the excited states are labelled by f. This sum rule is easily understood in classical terms. The left-hand side is the average energy given to the nucleus by the collision. On the right-hand side, $\vec{\nabla}V(r)$ is the impulse given to a target nucleon at position r. Thus $(\vec{\nabla}V(r))^2/2m$ is the average kinetic energy given to a nucleon at r, and the integral is the average total energy given to

the nucleus. Since the integral involves only the ground state density, it can be reliably computed and compared with the actual strength of a given vibrational excitation. The peak in Fig. 4 has about 75% of the strength for a quadrupole vibration; if it were monopole the sum rule would be exceeded.

By now the systematic behaviour of the quadrupole vibration has been thoroughly studied[11]. The mean frequency varies with mass number as $\omega \sim 63/A^{1/3}$ MeV/$\hbar$. The width varies from 8 MeV in light nuclei to 3 MeV in heavy nuclei, with dips at magic nuclei.

In the past two years, experiments have been done at smaller angles, where the monopole and quadrupole have different behaviour. Inelastic scattering at 0° should favour the monopole vibration. The physics behind this is shown in Fig. 5 which shows a projectile wave enveloping a nucleus. The attractive interaction between the projectile and the target pulls the nucleus out along the equatorial region. This outwards motion can be resolved into a major monopole component and a minor quadrupole component. All the wavelets from the projectile will interfere coherently at 0° scattering angle. So, like the Poisson spot seen in optical diffraction around spheres, the scattering will show a pronounced peak at 0°.

The quantum calculations of the scattering support this picture: Fig. 6 shows calculations comparing the angular distributions of monopole and quadrupole at the most forward angles[36]. These calculations treat the excitation of the vibration in the Born approximation, and use the solution of the Schrödinger equation in an optical potential for the projectile wavefunction. The sharp rise of the monpole near 0° is evident.

As the experiments have progressed to smaller angles with shorter wavelength projectiles, evidence has accumulated for a monopole vibration at a frequency slightly higher than the quadrupole. Figure 7 shows recent data (D. Youngblood, personal communication) for 0° inelastic α scattering. The centroid of the peak is at

$$\omega \sim 80/A^{1/3}\ (\mathrm{MeV}/\hbar)$$

Fortuitously, this is the same frequency as the dipole mode. The damping width of the vibration is about the same as for the quadrupole.

Theory

Paralleling the experimental developments, there have been considerable advances in the theory of the vibrations. The general theory, derived from many-body quantum mechanics in the 1950s, is known as RPA (random phase approximation). This theory was originally applied to nuclei[12,13] in models which used an oversimplified description of the wavefunction. These models were instructive in exhibiting qualitative trends for the vibrational frequencies but they had severe deficiencies. The sum rules were not satisfied. The interaction between particles was unrealistic, and in many cases had to be adjusted to fit observed vibrational properties. In the past decade it has become possible to do the theory properly. The availability of

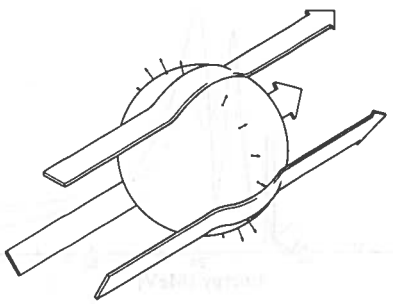

Fig. 5 A projectile wave, depicted with the broad arrows, envelops a nucleus and induces the transverse motion of the nucleus, shown with the small arrows. This motion resolves into a combination of monopole and quadrupole vibrations.

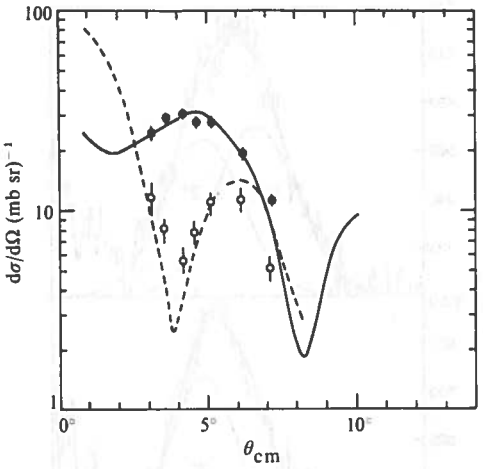

Fig. 6 Angular distribution for inelastic α scattering on ^{208}Pb (ref. 36). The solid line is the theoretical distribution for exciting a quadrupole vibration $E_x = 11.0$ MeV; $L = 2$, and the dashed line is the theoretical distribution for the monopole $E_x = 13.7$ MeV; $L = 0$. Points are data extracted by fitting the peaks like those in Fig. 4.

medium-sized computers means that the description of the wavefunction can be kept sufficiently general. In a configuration representation, the number of configurations for a heavy nucleus is typically several hundred. An example of an RPA calculation of the photon absorption strength is shown in Fig. 8[14]. The other key to a quantitative theory is the use of the same interaction hamiltonian to describe the vibrations as is used for the Hartree–Fock ground state. The important property of the interaction is that it contains a short range attraction which diminishes as the density increases. A simple parameterisation of the hamiltonian introduced by Skyrme has the form,

$$H = \sum_i \frac{p_i^2}{2m} + \sum_{i<j} v(n_0, \mathbf{p}_i, \mathbf{p}_j)\, \delta(r_i - r_j)$$

where v is a polynomial function of density $n_0(r)$ and momentum $\mathbf{p}_i$. Such a hamiltonian can be determined by fitting ground-state sizes and binding energies[16]. More fundamental theories of the interaction, based on the free nucleon–nucleon potential, can be reduced to the Skyrme form.[17] With the zero-range interaction, the Hartree–Fock ground states of nuclei are easily computed, as is the RPA response. With the largest computers, it is feasible to remove the restriction to zero-range interactions in the hamiltonian, and the most sophisticated RPA calculations are based on a more general parametrisation[18]. Using a hamiltonian consistent with ground state properties, the RPA gives an excellent description of the vibrations without any adjusted parameters[19]. The sum rules are automatically satisfied. The giant vibrations, with the exception of the monopole, are found at the proper frequency. The frequencies of low vibrations are generally reproduced to 10%. Figure 9 compares the theoretical[20] and experimental[19] density fluctuation in a low-frequency vibration of ^{208}Pb. Note that the density fluctuation is strongest at a radius ~7 fm, which is at the nuclear surface.

The RPA can be simplified to algebraic formulae when the vibration exhausts the sum rule. These formulae are analogous to the classical formula for a vibrational frequency ω in terms of a mass M and spring constant k, $\omega^2 = k/M$. Before the RPA theory was known, classical models were proposed *ad hoc*. In the case of the dipole vibration, the mass is simply the mass of the protons and neutrons. The restoring force is due to the change in potential energy when the protons and neutrons are displaced with respect to each other. The dipole frequency was first calculated along these lines by Migdal in 1944 (ref. 22; see also refs 23. 24). The dipole motion in Fig. 1 physically separates neutrons from protons in the surface region: Migdal modified

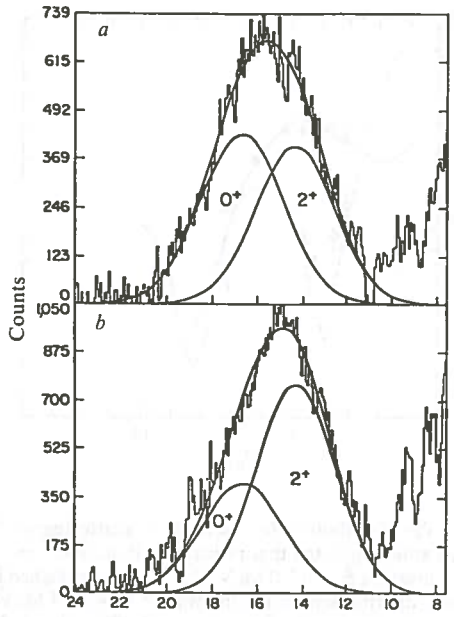

Fig. 7 Comparison of the α scattering at *a*, 0°; and *b*, 4°. The peak is shifted upward in energy at 0°, due to the relative enhancement of the monopole at the forward angle.

the velocity fields to keep the particles together at the surface. The predicted frequency is then found to be

$$\omega \sim \left(\frac{4.3 b_s}{MR^2}\right)^{1/2} \sim 80/A^{1/3}\ (\mathrm{MeV}/\hbar) \qquad (1)$$

where $b_s \simeq 50$ MeV is the symmetry energy of nuclear binding. The reduction of RPA yields a formula that contains additional factors arising from mesons and from a more accurate description of the velocity field[25,26]. These corrections tend to cancel, and equation (1) is in excellent agreement with the empirical vibration frequencies of the heavier nuclei.

Migdal[22] and others[27] also tried to calculate the quadrupole vibrational frequency, but in this case the classical ideas were simply wrong. It was assumed that the surface tension of the nuclear surface provided the restoring force to the spherical shape. The general formula for liquid drop vibrations was derived by Rayleigh, and is

$$\omega^2 = \frac{\sigma n_0}{MR^3} L(L-1)(L+2)$$

where σ is the surface tension. The formula can be evaluated using the nuclear surface tension derived from binding energy systematics. The predicted frequency is found to be ~2 MeV for heavy nuclei, which is much too low[27]. However, as mentioned above, RPA calculations do predict the quadrupole vibration at the correct frequency. In fact, on the basis of such calculations Mottelson in the 1960s urged a search for the mode.

The reason why the classical calculation fails is that the main element in the restoring force is neglected. There is a resistance to shearing motion in any Fermi system caused by the complex spatial structure of the many-Fermion wavefunction. It turns out that the elastic shear modulus is proportional to the quantum kinetic energy of the particles. The proper formula for the vibrational frequency based on this restoring force is

$$\omega^2 = \frac{2\langle T\rangle}{M\langle r^2\rangle} \qquad (2)$$

Here $\langle r^2\rangle$ is the mean square radius of the ground state, and $\langle T\rangle$ is the average kinetic energy per particle in the nucleus. Note that this formula, unlike the liquid drop formula, has the correct $A^{-1/3}$ dependence of frequency on mass number because $\langle r^2\rangle \sim A^{2/3}$. When a simple estimate is made of the kinetic energy per particle, for example, with the Fermi gas model or harmonic oscillator model, the predicted frequency from equation (2) agrees with the empirical model to better than 10%. As in the case of the dipole, equation (2) is somewhat oversimplified, since some of the subtler effects of the nuclear interactions are neglected[28].

We now consider the theory of the most recently discovered giant vibration, the monopole. The frequency of the monopole is especially interesting because it is directly related to the compressibility of nuclear matter. The compressibility is a fundamental property of the medium, but up to now there has been no way to measure it. There have been many calculations of nuclear compressibility beginning in the early 1940s, before the nuclear interaction was very well known. Techniques of calculations have since become very sophisiticated, but we do not yet have a satisfactory understanding of the equilibrium density of nuclear matter[29]. More detailed properties of the nuclear medium, such as its compressibility, are correspondingly more difficult to calculate. However, the existing calculations should serve as a guideline. Predicted values for the compressibility are in the range

$$k = V^2 \frac{\partial^2 E}{\partial V^2} = 2.5\text{–}5\ (\mathrm{MeV\,fm^{-3}})$$

with the higher number being more recent. The classical relationship between the radial vibration frequency and the compressibility of a liquid drop is $\omega^2 = \pi^2(k/Mn_0R^2)$. Applying this formula to finding k from the empirical ω, the compressibility of nuclear matter turns out to be $k \approx 3.5$ MeV fm^{-3}. Having fixed the compressibility coefficient with the information from the monopole, it will now be possible to make more reliable calculations of other phenomena involving high-density nuclear matter. This includes high-energy heavy-ion collisions and the formation of neutron stars.

Damping

The damping of the nuclear vibrations is not well understood, theoretically or experimentally. There are two possible mechanisms for the damping. The vibration may disappear by emitting particles, which could be called evaporation; or the motion may mix with the more complex degrees of freedom in the many body system, which is analogous to friction. This complex state would eventually decay according to statistical considerations, which generally emphasise low-energy neutron emission. The measurement of decays of giant vibrations is a very active area of research. Some published experiments in the heavier nuclei claim that the decays are inconsistent with the statistical picture[30,31]. On the theoretical side, the damping by particle emission is found to be unimportant except in light nuclei. In RPA, the damping rate due to nucleon emission can be

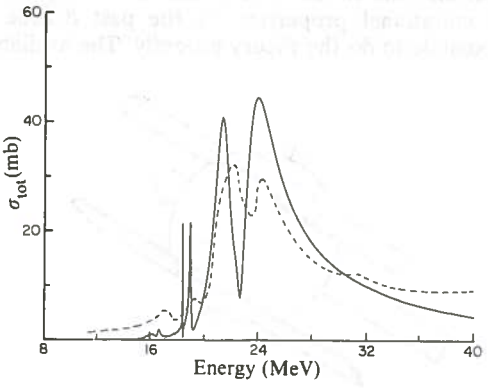

Fig. 8 The photon absorption strength of ^{16}O in the RPA theory (solid line)[14], compared with experiment (dashed line). The resonance is split into five components by the shell structure, and has a width due to the decay by nucleon emission.

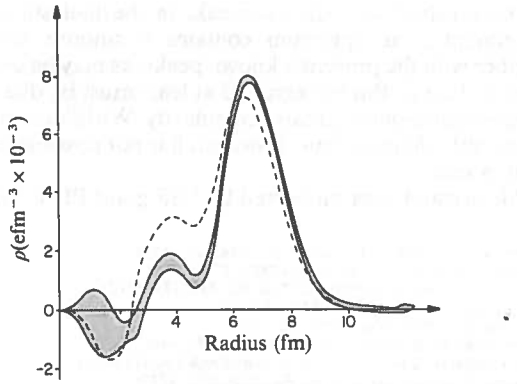

Fig. 9 The transition charge density $\langle 3^-|\rho|0^+\rangle$ for the lowest $L=3$ state in ^{208}Pb. The experimental density[20] (hatched area) is measured by a Fourier–Bessel transform of the electron scattering form factor. The theoretical density[19] is the result of an RPA calculation (dashed line), using a large basis for the wavefunction but a simple interaction.

calculated directly[14,15]. The rate of emission of heavier particles, such as α particles, is more difficult to calculate but is also estimated to be small.

Nevertheless, the study of emitted particles has provided a useful tool for studying the vibrations. By examining a particular final transition, the emitted particle can be forced to carry away the entire angular momentum of the vibration. If a coordinate system is chosen in which there is no angular momentum about the z axis, the angular distribution of the particle then follows a Legendre function, $N(\theta) \approx (P_L(\theta))^2$.

Such a measurement was made for the giant quadrupole of ^{16}O, decaying by α-particle emission to the states in ^{12}C (ref. 32). The angular distribution for the ground tate transition, which satisfies the above condition, is shown ı Fig. 10. The data exhibit a peak at 0° of the right width to be described by $[P_2(\theta)]^2$. However, unlike the Legendre function, the data is not symmetric about 90°. This means there must be coherent mixtures of angular momenta. The fact that the background interferes with the decay of the vibration is not really unexpected. In the classical limit nucleon emission can take place by the projectile's knocking out a nucleon in the direction of the momentum transfer. The quantum description of this process requires intereference from many angular momenta. It remains to be seen what theory predicts about how much interference is required.

The other form of damping is caused by mixing with more complicated modes of motion. A simple example of this is the behaviour of the dipole state in a deformed nucleus. A vibration in an arbitrary direction resolves into vibrations along the principal axes with different frequencies. This is seen in Fig. 11, showing the dipole strength for an ellipsoidal nucleus.

The lineshape can be well described as the sum of two lorentzian curves. The lower frequency and higher frequency components correspond to the vibration along the major and minor axes respectively. The difference in frequencies agrees well with the R dependence in equation (1). Because there are two minor axes, the upper peak is predicted to have twice the strength which is found to be the case empirically. For the quadrupole vibration, there are three distinct frequencies instead of two, and the overall splitting is smaller because the motion has components along both principal axes. Consequently, for the quadrupole the deformation splitting is much more difficult to see.

The major source of damping is mixing with the statistical degrees of freedom of the many body system. In principle, this could be calculated from the shell model representation of nuclear wavefunctions, and several calculations along such lines have been reported[33,34]. However, these calculations are not transparent, and it is more instructive to ask how the damping of the vibrations compares with damping of other kinds of motion.

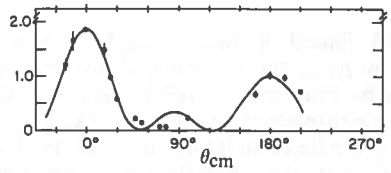

Fig. 10 Angular distribution of decay α particles following excitation of ^{16}O in the giant quadrupole region[32]. The 0° axis is along the momentum transfer direction. The probability distribution peaks in this direction, and also has a smaller peak in the opposite direction. $E_x = 17.9$–19.2 MeV.

The simplest motion is that of a single nucleon across the nucleus. This is described quantum mechanically with an optical potential, and the finite lifetime of the nucleon τ is related to the imaginary part of the optical potential $\langle W\rangle$ by $\hbar/\tau = 2\langle W\rangle$. Optical potentials can be inferred from elastic scattering of low energy nucleons and from the capture of neutrons. The spreading of the single-particle strength can also be seen directly in the reactions in which a nucleon is transferred between the projectile and the target. These methods yield a damping width for nucleons close to the particle emission threshold of about $\hbar/\tau \approx 5$ MeV.

A naive model of the vibrational damping can then be constructed, utilising the representation of the wavefunction in terms of single-particle wavefunctions. The vibration is a superposition of one particle above the Fermi level together with a hole in the Fermi sea. Each of these should have a single particle lifetime so the total damping width would be twice that, hence $\hbar/\tau \approx 10$ MeV.

This estimate ignores a coherence in the vibrational motion: the fact that all of the particles are moving together inhibits the coupling to other degrees of freedom. This coherence is well-known in other quantum systems. For example, in metals the plasmon vibration might only be damped by 1 eV while an electron at the same energy has a damping many times larger. In fact, the detailed calculations of nuclear vibrational damping do show this quenching effect[35].

Although classical ideas are relevant to the description of the vibrational frequencies, they have not yet been helpful in discussions of damping. The classical concept for dissipation in extended systems is viscosity, and attempts have been made to apply this idea to the nuclear vibrations. Unfortunately, there is no fundamental justification for viscosity; it is only valid when particles have short mean free paths. In nuclei, the particles can travel completely across the nucleus with a high probability. The nuclear surface probably plays a more important part in the damping than do collisions between particles in the interior. A simple description of the damping in these circumstances is needed not only for the understanding of nuclear vibrations, but also for interpretation of data on heavy ion collisions.

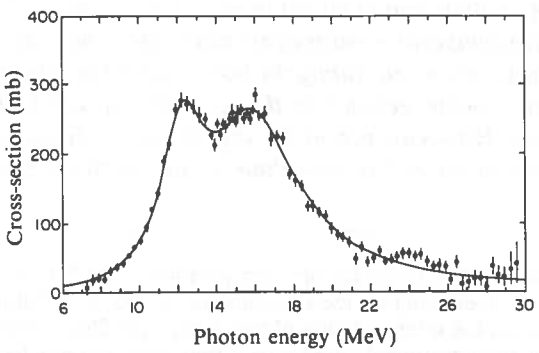

Fig. 11 The giant dipole resonance is ^{150}Gd, an ellipsoidal nucleus (ref. 3, Fig. 28). The curve is a sum of two lorentzian functions, the upper having twice the area of the lower.

Prospects

What is the likelihood of discovering more vibrations? The possibility of more complex motion always exists, and other vibrations can be calculated in RPA. However, all the other modes of particle displacement have a higher mean frequency. The damping is predicted to be much larger, both within RPA and due to the coupling to other degrees of freedom. Thus it is unlikely that a coherent mode, containing most of the sum rule, will be resolved as a distinct peak. In the inelastic scattering experiments, the spectrum contains a smooth background together with the presently known peaks, as may be seen in Figs 3 and 4. Part of this background at least must be due to highly damped vibrations of greater complexity. Without some specific measurable characteristic, however, it is not possible to identify them as such.

This research was supported by NSF grant PHY 7620097.

1. Bothe, W. & Gentner, W. *Z. Phys.* **106,** 236 (1937); **112,** 45 (1939).
2. Baldwin, G. & Klaiber, G. S. *Phys. Rev.* **73,** 1156 (1948).
3. Berman, B. L. & Fultz, S. C. *Rev. Mod. Phys.* **47,** 713 (1975).
4. Panofsky & Phillips, *Classical Electricity and Magnetism*, 335 (Addison-Wesley, New York, 1955).
5. Levinger, J. S. & Bethe, H. A. *Phys. Rev.* **78,** 115 (1950).
6. Tyren, H. & Maris, Th. A. J. *Nucl. Phys.* **4,** 637 (1957).
7. Lewis, M. B. & Bertand, F. E. *Nucl. Phys.* **A196,** 337 (1972).
8. Pitthan, R. & Walcher, T. *Phys. Lett.* **36B,** 563 (1971).
9. Youngblood, D. H. *et al. Phys. Rev.* **C13,** 994 (1976).
10. Bernstein, A. M. *Adv. Nuc. Phys.* **3,** 325 (1969).
11. Betrand, F. E. *A. Rev. Nucl. Sci.* **26,** 457 (1976).
12. Baranger, M. *Phys. Rev.* **120,** 957 (1960).
13. Brown, G., Evans, J. & Thouless, D. *Nucl. Phys.* **24,** 1 (1961).
14. Shlomo, S. & Bertsch, G. *Nucl. Phys.* **A243,** 507 (1975).
15. Krewald, S. *et al. Phys. Rev. Lett.* **33,** 1386 (1974).
16. Vautherin, D. & Brink, D. *Phys. Rev.* **C5,** 626 (1972).
17. Negele, J. & Vautherin, D. *Phys. Rev.* **C5,** 1472 (1972).
18. Blaizot, J. P. & Gogny, D. *Nucl. Phys.* **A284,** 429 (1977).
19. Bertsch, G. & Tsai, S. F. *Phys. Rep.* **18C,** 127 (1975).
20. Speth, J., Werner, E. & Wild, W. *Phys. Rep.* **33C,** 127 (1977).
21. Rothhaas, H. *et al. Phys. Lett.* **51B,** 23 (1974).
22. Migdal, A. *J. Phys.* (Moscow) **8,** 331 (1944).
23. Goldhaber, M. & Teller, E. *Phys. Rev.* **74,** 1046 (1948).
24. Steinwedel, H. & Jensen, J. A. D. *Z. Naturforsch.* **5A,** 413 (1950).
25. Myers, W. & Swiatecki, W. *Phys. Rev.* **C15,** 2032 (1977).
26. Bertsch, G. & Stricker, K. *Phys. Rev.* **C13,** 1312 (1976).
27. Bohr, A. & Mottelson, B. *Kgl. Dan. Vid. Selsk. Med.* **27,** No. 16 (1953).
28. Golin, M. & Zamick, L. *Nucl. Phys.* **A249,** 320 (1979).
29. Day, B. D. *Rev. Mod. Phys.* **50,** 495 (1978).
30. Wolynec, E., Dodge, W. R. & Hayward, E. *Phys. Rev. Lett.* **42,** 27 (1979).
31. van der Plicht, J. *et al. Phys. Rev. Lett.* **42,** 1121 (1979).
32. Knöpfle, K. T. *et al. Phys. Lett.* **74B,** 191 (1978).
33. Danos, M. & Greiner, W. *Phys. Rev.* **B138,** 876 (1965).
34. Soloviev, V. G., Stoyanov, C. & Vdovin, A. *Nuc. Phys.* **A288,** 376 (1977).
35. Bertsch, G. *et al. Phys. Lett.* **80B,** 161 (1979).
36. Youngblood, D. H. *et al. Phys. Rev. Lett.* **39,** 1188 (1977).

articles

A 30,000-yr isotope climatic record from Antarctic ice

C. Lorius*, L. Merlivat†, J. Jouzel† & M. Pourchet*

* Laboratoire de Glaciologie du CNRS, 2, rue Très Cloïtres 38031 Grenoble Cedex, France

† Laboratoire de Géoisotopie de l'Eau, DRA Saclay, B.P. 2, 91190 Gif/Yvette, France

Simple glaciological conditions at Dome C in east Antarctica have made possible a more detailed and accurate interpretation of an ice core to 950 m depth spanning some 32,000 yr than that obtained from earlier ice cores. Dated events in comparable marine core has enabled the reduction of accumulation rate during the last ice age to be estimated. Climatic events recorded in the ice core indicate that the warmest Holocene period in the Southern Hemisphere occurred at an earlier date than in the Northern Hemisphere.

ALTHOUGH the stable isotopic composition ($^{18}O/^{16}O$, D/H) of polar ice sheets can provide a continuous record of past climatic conditions, the interpretation of the isotope profiles in terms of climatic temperature changes over a time scale ranging back to the last ice age is complicated by several factors including: (1) the determination of the time scale; (2) the influence of the elevation at which the snow was deposited and of ice sheet stability; (3) the establishment of a transfer function from isotopic δ ratio to temperature in past conditions. Despite these limitations the study of ice cores has already provided very useful palaeoclimatic data[1–5]. Similar limitations occur in the interpretation of other indirect sources of climatic data.

As isotopic records from areas near an ice divide are simpler to interpret, thermal core drilling to 906 m depth was carried out at Dome C (74° 39′ S; 124° 10′ E; elevation: 3,240 m, mean annual temperature: −53.5 °C, Fig. 1) during the 1977–78 Antarctic field season as part of the International Antarctic Glaciological project[6].

The isotope profile

The core recovery was about 98%. Sampling was carried out in the field by cutting a continuous slice from along the length of cleaned ice core. The $^{18}O/^{16}O$ ratios were measured with a fully automatic double mass spectrometer with an accuracy of 0.15‰ in the δ scale relative to the V. SMOW. The results averaged for samples of about 4 m length are plotted in Fig. 2 with depths expressed in metres of ice equivalent to take account of the

0028-0836/79/340644-05$01.00